HHS Public Access

Author manuscript

Neuromuscul Disord. Author manuscript; available in PMC 2024 March 01.

Published in final edited form as:

Neuromuscul Disord. 2023 March ; 33(3): 257–262. doi:10.1016/j.nmd.2022.12.014.

MYH2-associated Myopathy Caused by a Novel Splice-Site Variant

Thomas A. Cassini[1], **May Christine V. Malicdan**[2], **Ellen F. Macnamara**[2], **Tanya Lehky**[3], **Iren Horkayne-Szakaly**[4],

Undiagnosed Diseases Network,

Yan Huang[2], **Robert Jones**[4], **Rena Godfrey**[2], **Lynne Wolfe**[2], **William A Gahl**[2,5], **Camilo Toro**[2]

[1]Medical Genetics & Genomic Medicine Training Program, National Human Genome Research Institute (NHGRI), NIH, Bethesda, Maryland, USA

[2]NIH Undiagnosed Diseases Program, Common Fund, NIH, Bethesda, Maryland, USA

[3]EMG Section, National Institute of Neurological Disorders and Stroke, National Institutes of Health, Bethesda, MD 20892, USA

[4]The Joint Pathology Center, Defense Health Agency, Silver Spring, MD 20910, USA

[5]Office of the Clinical Director, National Human Genome Research Institute (NHGRI), NIH, Bethesda, Maryland, USA

Abstract

MYH2 encodes MyHCIIa, a myosin heavy chain found in fast type 2A fibers. Pathogenic variants in this gene have previously been implicated in dominant and recessive forms of myopathy. Three individuals reported here are part of a family in which four generations of individuals are affected by a slowly progressive, predominantly proximal myopathy in an autosomal dominant inheritance pattern. Affected individuals in this family lacked classic features of an *MYH2*-associated myopathy such as congenital contractures and ophthalmoplegia. A novel variant, *MYH2* c.5673+1G>C, was detected in the proband and subsequently found to segregate with disease in five additional family members. Further studies demonstrated that this variant affects splicing, resulting in novel transcripts. These data and muscle biopsy findings in the proband, indicate that this family's *MYH2* variant is causative of their myopathy, adding to our understanding of the clinical and molecular characteristics of the disease.

Thomas A. Cassini is the corresponding author. thomas.cassini@nih.gov. Phone- (414) 531-3728. Fax- (301) 496-7157. Address: 9000 Rockville Pike, Bethesda, MD, 20892.

AUTHOR CONTRIBUTION

TC, MM, EM, and CT conceptualized and wrote the initial draft of the manuscript. TC, EM, RG, LW, and CT provided clinical care to the participants. MM, TL, HIS, YH, and RJ performed experiments, provided data interpretation and data analysis, and generated final figures. WAG is the PI of the lab and provided supervision. All authors have reviewed and approved the final version of this manuscript.

Declarations of interest: none

Keywords

Myopathy; MYH2; RNAseq; Splice-site; Undiagnosed Diseases Program

INTRODUCTION

Myosin is the major molecular motor protein in muscle. It is composed of a hexamer containing 2 heavy chains, each paired with 2 non-identical light chains. The heavy chain dimerization results in a polarized structure with a globular head domain at the amino terminus, which binds actin and hydrolyzes ATP, and a coiled-coil alpha helical structure at the carboxy terminus that mediates thick filament formation [1]. The heavy chains exist in several isoforms corresponding to different muscle types. The main isoform found in fast, type 2A fibers is MyHC-IIa, which is encoded by the gene *MYH2* [2].

MYH2 pathogenic variants were first implicated in 1998 as the cause of predominantly proximal muscle weakness and atrophy with external ophthalmoplegia [3,4]. The associated phenotype was previously referred to as hereditary inclusion-body myopathy-3 (IBM3). Onset is typically in adolescence or early adulthood and the course may be either slowly progressive or non-progressive. Additional features include facial weakness, tremors, and joint contractures at birth that sometimes resolve over time [4–6]. *MYH2* variants can lead to disease with an autosomal recessive or autosomal dominant inheritance pattern [5]. This is radiographically characterized by fatty infiltration of variable severity and muscle group involvement [6–8]. The histologic hallmark is small size, paucity, or absence of type 2A fibers selectively. Other findings may include dystrophic changes, minicores, intranuclear and cytoplasmic inclusions, rimmed vacuoles, filamentous tangles, and clusters of nemaline rods [9].

Here we describe a large, multigenerational family with late childhood or early adult-onset proximal muscle weakness without contractures or ophthalmoplegia segregating to a novel *MYH2* pathogenic variant at the donor splice site of the penultimate exon. The proband carried a clinical diagnosis of limb girdle muscular dystrophy but no genetic diagnosis. Due to the lack of a distinct diagnosis and the high prevalence of symptoms in her family, she sought an evaluation by the National Institutes of Health Undiagnosed Diseases Program (UDP) [10,11].

CASE REPORTS

Proband

The proband (Figure 1, IV-2) was a 49-year-old woman at the time of her initial evaluation by the UDP. She met her early motor developmental milestones at appropriate ages. Throughout childhood she noted difficulty with rising from a seated position and going up stairs. She remained physically active into her 4th decade of life, running 3–5 miles daily, but noted a gradual decline in her strength. By then, she also noted weakness in her arms, with difficulty reaching overhead. She had no visual symptoms, such as diplopia or ptosis.

She was evaluated by a neuromuscular specialist at age 46. Her evaluation included a creatine kinase (CK), electromyography (EMG), and magnetic resonance imaging (MRI) of her brain and spine, all of which were normal. A custom muscular dystrophy gene panel, evaluating 35 genes, revealed only a heterozygous variant of uncertain significant in the *SYNE1* gene, which was not thought to be the cause of her condition (Supplementary Appendix A).

On evaluation by the UDP, her muscle strength was 4+/5 in neck flexion, 5-/5 in shoulder abduction and adduction, 4+/5 in elbow extension, 4+/5 in wrist extension, and 4+/5 in hip flexion. Other muscles groups had 5/5 strength. Her eyed lids and extraocular movements were normal. The remainder of the neurologic exam was also normal. Her CK was normal at 72 U/L [normal range 39–308 U/L]. Her EMG study was consistent with a primary muscle disorder, most evident in the deltoid and biceps muscles with small, short duration motor unit potentials, some polyphasic units, and early recruitment. The leg muscles (vastus lateralis and medial gastrocnemius) had a mixed picture involving large motor unit potentials. Membrane irritability with the presence of fibrillation potentials and positive sharp waves was observed only in the proximal leg muscle (Supplementary Table 1). Muscle ultrasound showed diffuse muscle atrophy and hyperechogenicity most evident in the deltoid, triceps, quadriceps, and medial gastrocnemius. T1 MRI images of her lower extremities showed diffuse, symmetric, mild to moderate atrophy and fatty infiltration in the gluteal muscles. Thighs muscles demonstrated moderate fatty infiltration involving all muscles in the anterior and posterior compartment with relative sparing of the hip adductor and rectus femoris muscles. Posterior compartment involvement affected primarily the semitendinosus more than semimembranosus muscles (Figure 2A). TI inversion recovery (STIR) images did not suggest active myositis (not shown). An echocardiogram was normal.

Family history revealed a similar phenotype in an autosomal dominant inheritance pattern spanning 4 generations with at least 17 family members affected (Figure 1). The weakness largely did not impact the ability to complete activities of daily living, and developmental milestones were reached at typical ages. However, the family could accurately identify children who would eventually become clinically affected with distinct muscle weakness by noticing their strategy to rise from the floor or their inability to maintain the same level of activity as other children of the same age. The weakness affected mainly proximal muscles and was static or very slowly progressive over decades. No family members reported ophthalmoplegia or contractures.

There was a reported history of postural tremor of the upper extremities in several family members, but it did not segregate with the muscle weakness phenotype. None had significant cardiac or respiratory disease. Some, including the proband's mother, developed difficulties with ambulation late in life consistent with camptocormia or "bent spine" due to weakness of extensor paraspinal muscles. Two additional family members in the same generation as the proband underwent clinical evaluation.

Relative 1

Relative 1 (Figure 1; Individual IV-12), a 40-year-old man at the time of his evaluation by the UDP, reported his first symptoms around age 14–15, when his competitive distance

running time worsened. Still, 10 years later, he was able to run at least 5 miles per day. With higher intensity exercise he noticed diffuse myalgia and had elevated CK blood levels up to 1200 U/L. Recently, he noted that his feet were slapping as he walked, and he developed arm weakness when lifting objects overhead. He had also received a diagnosis of “essential tremor”. This was a low amplitude, high frequency tremor. It began in his 20s and has progressed in severity. It is postural and exacerbated by movement, fatigue, and dehydration. He rarely drinks alcohol, but the tremor abates when he does. He has been treated with increasing doses of propranolol with good response. He had no visual symptoms.

Neurologic evaluation revealed strength to be 5-/5 in neck flexion, 5-/5 in shoulder abduction, 4+/5 in elbow extension, 5-/5 in wrist extension, 5-/5 in intrinsic muscles of the hands, 4+/5 in hip flexion, 5-/5 in hip extension, 5-/5 in foot dorsiflexion, and 4-/5 in toe extension with other muscle groups being 5/5. The remainder of his neurologic exam was normal. CK was normal at 151 U/L [normal range 39–308 U/L]. EMG showed a mixed pattern of small and large motor unit potentials with normal recruitment and without evidence of membrane irritability such as positive sharp waves or fibrillation potentials, not clearly diagnostic of a myopathic disorder (Supplementary Table 1). A primary muscle disorder with secondary neurogenic findings was suggested. T1 weighted MRI imaging of the lower extremities, like the proband, revealed diffuse, symmetric fatty infiltration of thigh musculature with relative sparing of the hip adductor and rectus femoris. Images of the calf musculature revealed atrophy and fatty infiltration of the medial head of the gastrocnemius, with less involvement of the soleus (Figure 2A).

Relative 2

Relative 2 (Figure 1; Individual IV-15) was a 37-year-old man at the time of his UDP evaluation. He had longstanding weakness first noticed in his quadriceps in high school when he expended considerable time and effort weightlifting. Despite 7 months of consistent strength training, he increased his ability to lift by only about 5 lbs. He had a mild tremor but no visual symptoms.

Neurologic examination revealed strength to be 5-/5 in neck flexion, 5-/5 in elbow flexion, 4+/5 in elbow extension, 5-/5 in wrist flexion, and 5-/5 in hip flexion with 5/5 strength in other muscle groups. The remainder of his neurologic exam was normal. CK was mildly elevated at 402 U/L [normal range 39–308 U/L]. EMG showed large motor unit potentials in the distal leg muscles (medial gastrocnemius and tibialis anterior) and proximal arm muscles (biceps and triceps) with some membrane irritability including positive sharp waves and fibrillation potentials in most muscles sampled (Supplementary Table 1). MRI of the lower extremities showed mild symmetric fatty infiltration and atrophy of the quadriceps but with rectus sparing of the femoris. Posterior compartment involvement affected primarily the semitendinosus more than semimembranosus. (Figure 2A).

Sequencing

Exome sequencing performed on the proband revealed the heterozygous variant NM_017534.6(*MYH2*):c.5673+1G>C (GRCh37) (Supplementary Appendix B). This variant is not reported in gnomAD and occurs on a canonical splice donor site of exon 39, which

may escape nonsense mediated decay or result in exon skipping by as predicted by silico tools. The same change was found in both relatives described above, as well as in her affected mother (3-III) and another affected cousin (IV-16). This change was not seen in her unaffected sister (IV-3), brother (IV-4), or cousin (IV-9).

Muscle Biopsy

Muscle biopsy of right vastus lateralis was performed on the proband at age 52 (Figure 2B). The formalin fixed biopsy revealed almost complete lack of type 2 myofibers in approximately 2/3 area of the biopsy specimen, highlighted by fast and slow myosin immunostaining. Similar features appeared to be present in the frozen biopsy specimen stained with ATPases at pH 10.4 and pH 4.6, but interpretation was limited due to the relatively small size of the specimen. Rare pyknotic nuclear clumps were noted. Esterase and nicotinamide adenine dinucleotide-tetrazolium reductase preparations highlighted the sarcoplasm of rare angular atrophic myofibers, consistent with denervation. Occasional swollen, hyalinized myofiber and myofibers with disrupted integrity of the membrane were noted, indicating degeneration. Occasional regenerating myofibers were also noted. Gomori trichrome stain was negative for ragged red fibers, rimmed vacuoles, sarcoplasmic inclusions, or nemaline rods. There was no evidence of an inflammatory process, metabolic myopathy or changes suggestive of mitochondrial abnormalities. In summary, the most prominent features were the small type 2 myofibers involving some of the fascicles, and very tiny and markedly lost type 2 fibers in the adjacent fascicles accompanied by denervation atrophy and mild myopathic changes.

Reverse Transcriptase Polymerase Chain Reaction (RT-PCR)

To further evaluate the impact of the variant on splicing, cDNA from patient-derived dermal fibroblasts was analyzed (Supplementary Appendix B). Bulk-RNA sequencing, performed on the proband's cells, showed aberrant splicing around exons 38 to 40 (Figure 3A). To confirm this, we performed RT-PCR on cDNA from the proband and affected relative (IV-13) using primers straddling exons 37 and 40. RT-PCR revealed the expected 402 bp band and two additional bands in the proband and her affected relative as compared to an unaffected individual (Figure 3B). To define the resulting sequence and splice alterations, we performed gel cloning followed by colony-PCR and sequencing. Sanger sequencing of clones revealed several isoforms (Figure 3C): normal; an isoform with skipping of exon 39; an isoform with intronic retention of 83 nucleotides; and an isoform with partial deletion of exon 37 and 38. Skipping of exon 39 (Figure 3D) is in-frame and will likely result in a shorter protein (c.5578_5673del; p.(Thr1860_Ala1891del)). The incorporation of an intronic segment led to an early termination codon (c.5473_5474ins83; p.(Val1825Glyfs*22)). Partial deletion of exons 37 and 38 also resulted an early termination codon (c.5394_5490del; p.(Asp1798Glufs*24)). These results support a functional effect of this variant that leads to aberrant splicing and the generation of an alternative transcript.

DISCUSSION

This family provides additional information regarding the phenotypic spectrum associated with deleterious variants in *MYH2*. This disorder may represent an under recognized and

underreported cause of myopathy since the clinical presentation is typically mild or static for prolonged time periods, unexpected to affect reproductive fitness and the molecular basis has only recently been implicated in disease. The family provided enough affected members that testing could definitively demonstrate segregation of the variant with disease, establishing strong evidence of pathogenicity.

Certain clinical aspects of the case stand out as distinct. First, none of the affected family members had ophthalmoplegia, which was previously described as a necessary feature to consider *MYH2* in the differential diagnosis. Only one case series prior to this described a family without ophthalmoplegia [5], but other reports suggested that the *MYH2* variant may not have been causative in that family and could have been simply a polymorphism [6]. The strength of evidence for the pathogenicity of the variant in this family expands the phenotype to include patients without ophthalmoplegia.

Second, this illustrates intrafamilial phenotypic variability. While family members typically share features of proximal muscle involvement, onset in childhood, and slow progression, there are other aspects that vary. For instance, some have more distal muscle affected as well as their proximal muscles and the pattern of this additional involvement varied. Additionally, some family members in this case have tremors, which have also been reported as an inconsistent feature in previous reports of this condition [4, 5]. Postural tremor is highly prevalent in the general population, and it is unclear if myopathy and tremor co-segregate in this family, especially since the emergence of tremor might occur later in life. Finally, while the muscle disease in this family follows a relatively mild course, it could impact function later in life as illustrated by the presentation of the proband's mother with a "bent spine" syndrome.

The molecular cause in this family is also novel, since the variant *MYH2* c.5673+1G>C has not previously been reported. Based on the clinical presentation, this was suspicious for the cause of their disease, although as discussed above, some features were atypical. The muscle biopsy provided additional evidence as the variation in fiber size and small type 2 fibers are consistent with previous reports [5–7,9,12,13]. Immunohistochemical staining for fast and slow myosin is unable to differentiate type 2A and 2B fibers however, and type 2 atrophy is less specific for *MYH2*-associated myopathy than type 2A fiber atrophy. Ultimately based on the current recommendations [14–17], this would meet PVS1_moderate, PM2_supporting, and PP1_strong meeting criteria for likely pathogenic based on guidelines from the American College of Medical Genetics (ACMG). A splicing impact is supported by subsequent experiments, in which the cDNA analysis obtained from affect individual's fibroblasts cell lines revealed alternative isoforms generated by the splice-site variant. This highlights the utility of RNAseq performed using fibroblasts. Given that the protein product of *MYH2*, MyHCIIa, forms a dimer, this raises the possibility that abnormal transcripts act could through dominant negative mechanisms to cause disease. Overall, the clinicopathologic data combined with the molecular findings in this case provide convincing evidence that the clinical presentation in this family is due to a novel *MYH2* pathogenic variant.

Supplementary Material

Refer to Web version on PubMed Central for supplementary material.

ACKNOWLEDGEMENTS

The authors would like to thank the patients and their families for participating in this study. This study is supported by the Intramural Research Program of the National Human Genome Research Institute and the NIH Office of the Director's Common Fund.

REFERENCES

[1]. Ruppel KM, Spudich JA. Structure-function analysis of the motor domain of myosin. Annu Rev Cell Dev Biol 1996;12:543–73. 10.1146/annurev.cellbio.12.1.543. [PubMed: 8970737]

[2]. Oldfors A Hereditary myosin myopathies. Neuromuscul Disord 2007;17:355–67. 10.1016/j.nmd.2007.02.008. [PubMed: 17434305]

[3]. Martinsson T, Oldfors A, Darin N, Berg K, Tajsharghi H, Kyllerman M, et al. Autosomal dominant myopathy: Missense mutation (Glu-706 → Lys) in the myosin heavy chain IIa gene. Proc Natl Acad Sci U S A 2000;97:14614–9. 10.1073/pnas.250289597. [PubMed: 11114175]

[4]. Darin N, Kyllerman M, Wahlström J, Martinsson T, Oldfors A. Autosomal dominant myopathy with congenital joint contractures, ophthalmoplegia, and rimmed vacuoles. Ann Neurol 1998;44:242–8. 10.1002/ana.410440215. [PubMed: 9708547]

[5]. Tajsharghi H, Thornell LE, Darin N, Martinsson T, Kyllerman M, Wahlström J, et al. Myosin heavy chain IIa gene mutation E706K is pathogenic and its expression increases with age. Neurology 2002;58:780–6. 10.1212/WNL.58.5.780. [PubMed: 11889243]

[6]. Cabrera-Serrano M, Fabian VA, Boutilier J, Wise C, Faiz F, Lamont PJ, et al. Adult onset distal and proximal myopathy with complete ophthalmoplegia associated with a novel de novo p.(Leu1877Pro) mutation in MYH2. Clin Genet 2015;88:573–8. 10.1111/cge.12552. [PubMed: 25529940]

[7]. Hernandez-Lain A, Esteban-Perez J, Montenegro DC, Dominguez-Gonzalez C. Myosin myopathy with external ophthalmoplegia associated with a novel homozygous mutation in MYH2. Muscle Nerve 2018; 55: E8–E10. 10.1002/mus.25365.

[8]. Tajsharghi H, Hilton-Jones D, Raheem O, Saukkonen AM, Oldfors A, Udd B. Human disease caused by loss of fast IIa myosin heavy chain due to recessive MYH2 mutations. Brain 2010;133:1451–9. 10.1093/brain/awq083. [PubMed: 20418530]

[9]. Madigan NN, Polzin MJ, Cui G, Liewluck T, Alsharabati MH, Klein CJ, et al. Filamentous tangles with nemaline rods in MYH2 myopathy: a novel phenotype. Acta Neuropathol Commun 2021;9:1–13. 10.1186/s40478-021-01168-9. [PubMed: 33402227]

[10]. Gahl WA, Mulvihill JJ, Toro C, Markello TC, Wise AL, Ramoni RB, et al. The NIH Undiagnosed Diseases Program and Network: Applications to modern medicine. Mol Genet Metab 2016;117:393–400. 10.1016/j.ymgme.2016.01.007. [PubMed: 26846157]

[11]. Gahl WA, Wise AL, Ashley EA. The undiagnosed diseases network of the National Institutes of Health: A National Extension. JAMA - J Am Med Assoc 2015;314:1797–8. 10.1001/jama.2015.12249.

[12]. Willis T, Hedberg-Oldfors C, Alhaswani Z, Kulshrestha R, Sewry C, Oldfors A. A novel MYH2 mutation in family members presenting with congenital myopathy, ophthalmoplegia and facial weakness. J Neurol 2016;263:1427–33. 10.1007/s00415-016-8154-8. [PubMed: 27177998]

[13]. Findlay AR, Harms MB, Pestronk A, Weihl CC. Homozygous recessive MYH2 mutation mimicking dominant MYH2 associated myopathy. Neuromuscul Disord 2018;28:675–9. 10.1016/j.nmd.2018.05.006. [PubMed: 29934118]

[14]. Abou Tayoun AN, Pesaran T, DiStefano MT, Oza A, Rehm HL, Biesecker LG, et al. Recommendations for interpreting the loss of function PVS1 ACMG/AMP variant criterion. Hum Mutat 2018;39:1517–24. 10.1002/humu.23626. [PubMed: 30192042]

[15]. Jarvik GP, Browning BL. Consideration of Cosegregation in the Pathogenicity Classification of Genomic Variants. Am J Hum Genet 2016;98:1077–81. 10.1016/j.ajhg.2016.04.003. [PubMed: 27236918]

[16]. Richards S, Aziz N, Bale S, Bick D, Das S, Gastier-Foster J, et al. Standards and guidelines for the interpretation of sequence variants: A joint consensus recommendation of the American College of Medical Genetics and Genomics and the Association for Molecular Pathology. Genet Med 2015;17:405–24. 10.1038/gim.2015.30. [PubMed: 25741868]

[17]. Tavtigian SV, Harrison SM, Boucher KM, Biesecker LG. Fitting a naturally scaled point system to the ACMG/AMP variant classification guidelines. Hum Mutat 2020;41:1734–7. 10.1002/humu.24088. [PubMed: 32720330]

[18]. Ramoni RB, Mulvihill JJ, Adams DR, Allard P, Ashley EA, Bernstein JA, et al. The Undiagnosed Diseases Network: Accelerating Discovery about Health and Disease. Am J Hum Genet 2017;100:185–92. 10.1016/j.ajhg.2017.01.006. [PubMed: 28157539]

[19]. Splinter K, Hull SC, Holm IA, McDonough TL, Wise AL, Ramoni RB. Implementing the Single Institutional Review Board Model: Lessons from the Undiagnosed Diseases Network. Clin Transl Sci 2018;11:28–31. 10.1111/cts.12512. [PubMed: 28945957]

Highlights

- Three individuals with myopathy and a novel *MYH2* splice-site variant
- Myopathy had autosomal dominant inheritance in a large four-generation pedigree
- EMG, muscle MRI, and muscle biopsy consistent with *MYH2*-associated myopathy
- RNAseq on fibroblasts demonstrated that the variant alters splicing
- Lack of ophthalmoplegia and congenital contractures expands the phenotype

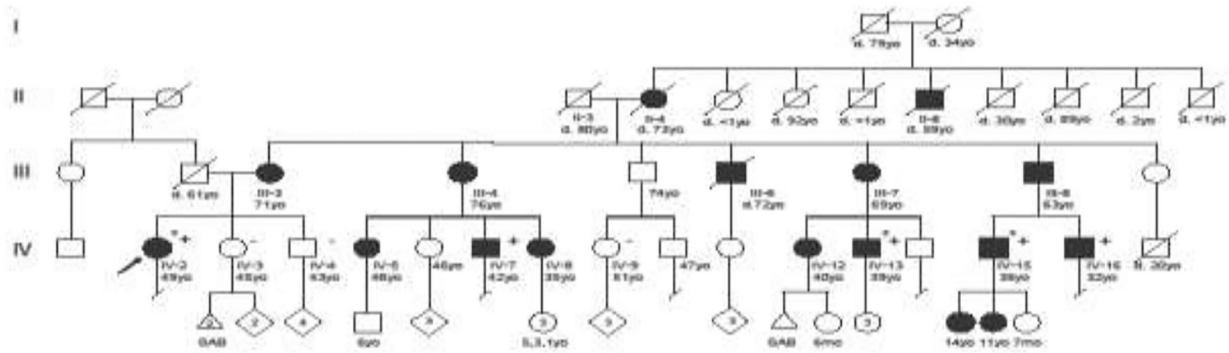

Figure 1. Family pedigree.

Pedigree at the time of proband evaluation showing family members affected (shaded) across four generations suggesting an autosomal dominant pattern of inheritance. Individuals evaluated by the UDP and reported here are marked with asterisks (*). Individuals who tested positive (+) and negative (−) for the familial variant are noted. “d.” denotes that the individual is deceased, and the number that follows is the age at death; yo, years old; mo, months old; SAB, spontaneous miscarriage.

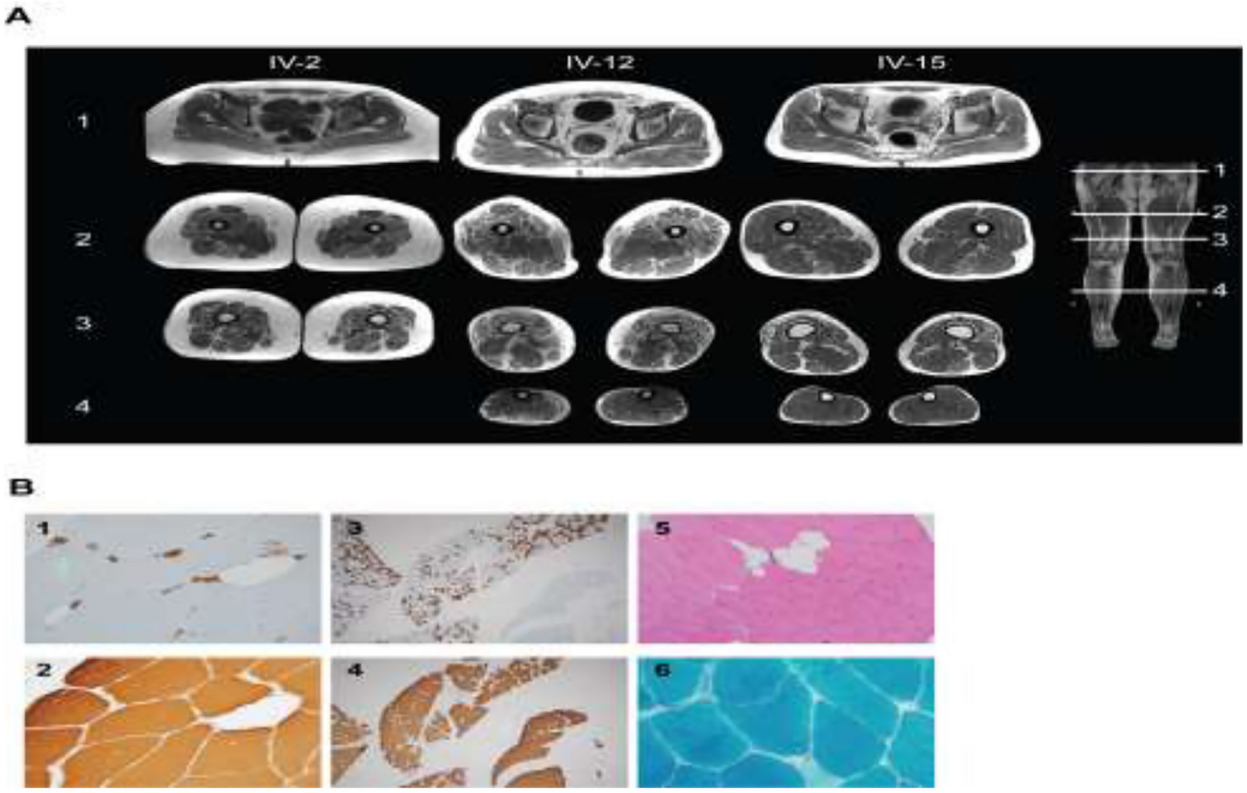

Figure 2. Muscle imaging and histology findings.

(A) Axial T1 MRI imaging of the lower extremities showing variable degrees of fatty infiltration and atrophy for three affected individuals (IV-2, IV-12 and IV-15) of this family. Images include axial sections at the level of the pelvis (1), proximal thigh (2), distal thigh (3), and calf (4). **(B)** Microscopic sections of the formalin fixed tissue show small type 2 myofibers highlighted by fast myosin immunohistochemical stain (1, 20x magnification). The same sections with slow myosin immunohistochemical stain demonstrate type 1 fibers with normal size and distribution (2, 20x magnification). Low magnification of the formalin fixed biopsy demonstrates that large areas of the muscle fascicles almost completely lack of type 2 myofibers, while other areas show small type 2 fibers with fast myosin staining (3, 2 × magnification). The same section stained by slow myosin shows normal size and distribution of type 1 myofibers. (4, 2 × magnification). H&E preparation reveals focal fat infiltration and rare pyknotic nuclear clumps (5, 40x magnification). Sarcoplasmic inclusions, nemaline rod or rod-like structures, filamentous tangles, ragged red fibers, or rimmed vacuoles are not seen on the Gomori trichrome stain (6, 40x magnification).

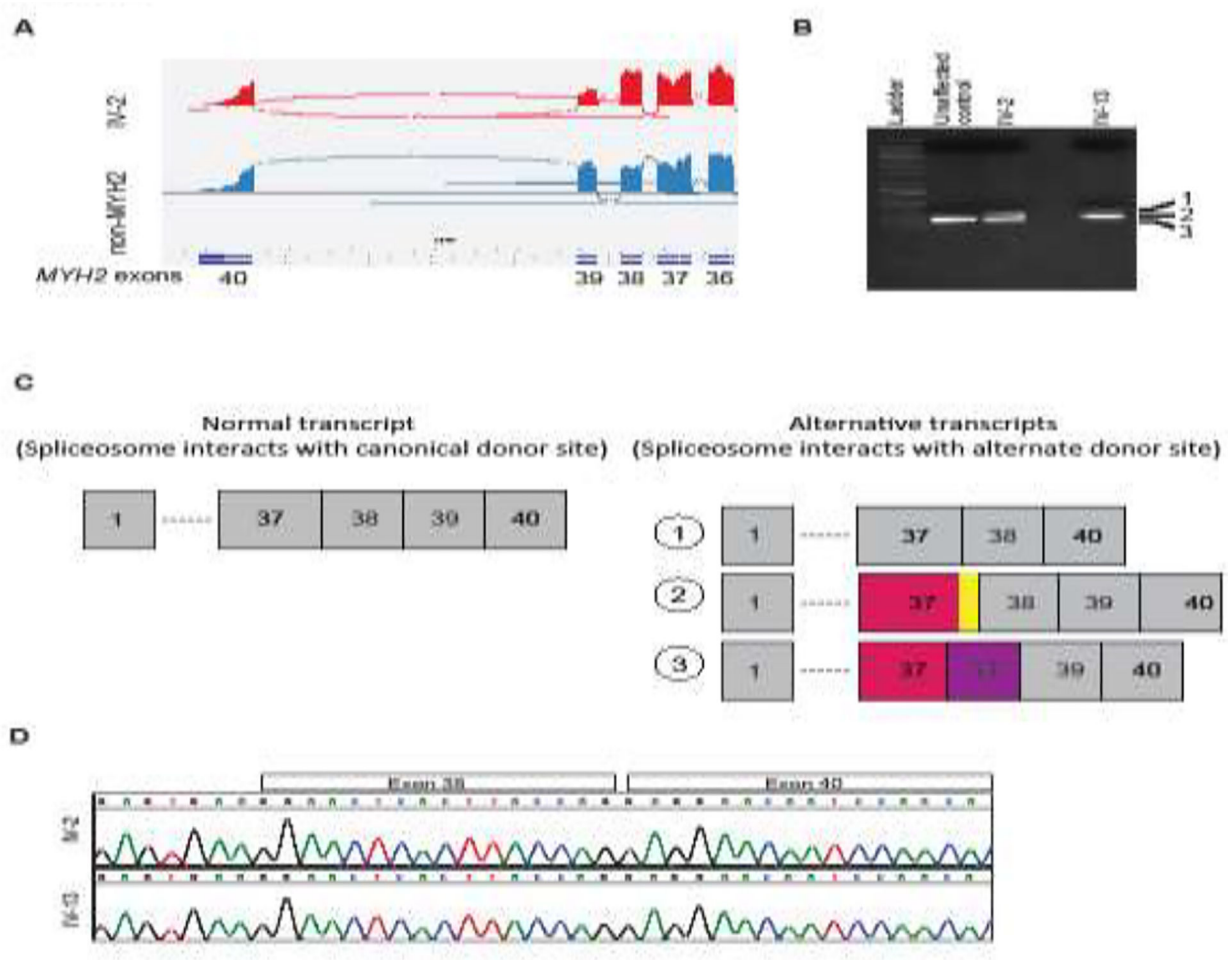

Figure 3. Consequences of the *de novo* MYH2 splicing variant.

(**A**) Sashimi plot of the proband's (IV-2) fibroblast RNA sequencing data compared to an individual without *MYH2* pathogenic variant (non-MYH2) using integrative genomics viewer (IGV). MYH2 is on a reverse orientation (3' to 5'). Note several reads from exon 38 to exon 40 of *MYH2*, suggesting exon skipping. (**B**) Reverse transcribed PCR of cDNA derived from proband (IV-2), affected relative (IV-13), and unaffected control. Primers straddling exons 37 to 40 showed the expected band in control, which is also seen in IV-2 and IV-13 (band 2). Additional bands are noted in IV-2 and IV-13 (bands 1 and 3), indicating abnormal transcripts. (**C**) A cartoon depicting a normal transcript of *MYH2* with 40 exons (left panel); exons 2–36 are not depicted to focus on exons 37–40. With the alternative donor site created by the *MYH2* variant in intron 39, at least three alternative transcripts are detected by cloning the bands and PCR products in (**B**). (**D**) Sanger sequencing reads to illustrate the in-frame skipping of exon 39.